

# Terahertz Generation from Quasi-Phase Matched Gallium Arsenide using a Type-II Ring Cavity Optical Parametric Oscillator

Patrick F. Tekavec<sup>a</sup>, Walter C. Hurlbut<sup>a</sup>, Vladimir G. Kozlov<sup>a</sup>, Konstantin Vodopyanov<sup>b</sup>

<sup>a</sup>Microtech Instruments, 858 West Park Street, Eugene, OR, USA 97401; <sup>b</sup>Dept. of Applied Physics, Stanford University, Ginzton Lab., Stanford, CA USA 94305-4088

## ABSTRACT

Resonant cavity enhancement results in substantial improvement in the efficiency of photonic THz-wave generation via difference frequency generation (DFG). A nearly degenerate optical parametric oscillator (OPO) was pumped by 6 ps pulses at 1064 nm, producing signal and idler pulses with average total power in excess of 80 W. By placing a sample of quasi-phasematched gallium arsenide (QPM-GaAs) at a focus of a ring cavity OPO, multicycle, narrowband THz radiation was produced, with average powers in excess of 100  $\mu$ W and peak powers exceeding 150 mW. The dependence of the THz power on pump power shows no signs of saturation, so with higher power pump lasers, mW levels of average THz should be obtainable.

**Keywords:** THz, GaAs, OPO

## 1. INTRODUCTION

High power, narrow linewidth THz sources are of particular interest in applications where long distance propagation through air is required. Photonic generation of THz radiation in electro-optic crystals via optical rectification (OR) and difference frequency generation (DFG) is a well-established method to produce such sources. However, due to the large difference between the optical pump and generated THz photons, this process is inherently low in efficiency (on the order of  $10^{-5}$ ) [1]. In order to produce high THz power, it is important to maximize the optical pump power, as well as to choose an optimal non-linear medium for the downconversion process. Resonant enhancement is a well-known technique to increase the power in nonlinear processes, and here we apply this to difference frequency generation. In previous work[ref], a QPM-GaAs crystal was placed inside a near-degenerate, doubly resonant periodically poled lithium niobate (PPLN) based OPO. Designs using type-II interactions (signal and idler perpendicular, pump polarized parallel to signal) in an offset linear cavity[2], and type-0 (all polarizations parallel) in a ring cavity [3] have been used in the past. While the type-0 design allows access to the higher nonlinear coefficient of PPLN and lower roundtrip loss, the broad acceptance bandwidth near degeneracy makes single line pair (signal and idler) operation difficult. The type-II OPO is more conducive to single line pair operation, but higher loss leads to lower intracavity powers. Here we use a type-II OPO with a ring cavity configuration, which allows us to take advantage of the single line pair operation of the type-II interaction, while avoiding the higher loss and complexity of the off-set linear cavity.

## 2. RING CAVITY OPO

A Fianium FP1060-10-CST Yb-fiber laser (1063.5 nm, 109 MHz, 6 ps, average power of 5 W) synchronously pumps the ring-cavity OPO (fig. 1). The OPO consists of mirrors, all highly reflecting ( $R > 99.9\%$ ) from 2.0  $\mu$ m – 2.2  $\mu$ m and highly transmitting ( $T > 90\%$ ) for the pump beam. The curved mirrors M1 and M2 have radius of curvature of 200mm, M4 and M5 have radius of curvature 500mm, M3 and M6 are flat. The gain medium for the OPO is a 10 mm long MgO doped PPLN crystal designed for type-II phase matching. The crystal was mounted in an oven for temperature tuning of the signal and idler frequencies. GaAs samples (AR coated at 2.1  $\mu$ m) were placed at the second focus on the cavity (between M4 and M5), and the THz radiated was reflected out of the cavity by a gold coated, off-axis parabolic mirror (OAP). A small hole (3 mm diameter) was drilled in the OAP to allow signal and idler to circulate.

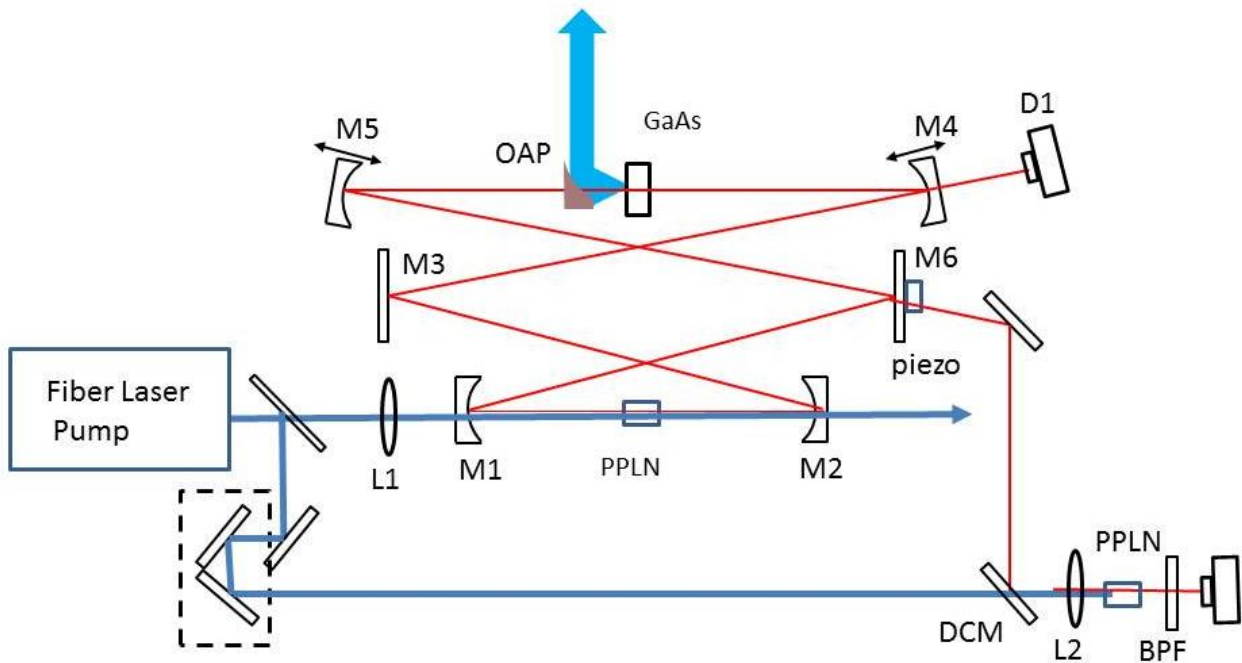


Figure 1. OPO setup. M1 and M2 curved mirrors  $R = 200$  mm. M4 and M5 curved mirrors  $R = 500$  mm. CB = birefringence compensation block. W = wedges. DCM = dichroic mirror. L1, L2, lenses. OAP = off-axis parabolic mirror. BPF = bandpass filter. D1 = InGaAs photodiode. D2 = Si photodiode. FCS = fiber coupled spectrometer.

For synchronous pumping, the optical path length of the OPO must match the repetition rate of the pump laser. For course adjustment of the cavity length, M4 and M5 are mounted on computer controlled translation stages, which can be adjusted to bring the cavity into resonance. However, since the signal and idler are orthogonally polarized, they experience a different index of refraction when passing through the gain crystal, and thus a different optical path length. To compensate for the birefringence of the gain crystal, compensation blocks of lithium niobate with  $c$ -axis rotated by 90 degrees with respect to the gain crystal are inserted in the cavity (not shown in figure). While the signal is an o-wave in the gain crystal, it is an e-wave in the compensation block, with the opposite being true for the idler. This configuration gives an equal net optical path for both beams, allowing both to resonate simultaneously. For a doubly resonant OPO, small changes in path length lead to large changes in circulating power. Stability was achieved in two ways: thermo-optics feedback from the GaAs crystal and feedback electronics. The thermo-optic effect is a negative feedback mechanism, which counteracts changes in the cavity length, thus stabilizing the cavity [4]. Electronic feedback is employed with a locking circuit that uses the output of the D1 to drive a piezo mounted on M6 for active stabilization of the cavity.

Tuning of the OPO was done by sequentially changing the temperature of the PPLN gain crystal and then adjusting the cavity length for maximum circulating power. The spectrum was measured by looking at the IR power leaking through M3 with a fiber coupled InGaAs spectrometer. Figure 2 shows the tuning curve of the signal and idler as a function of the PPLN temperature. Degeneracy occurs at a temperature of  $111^{\circ}\text{C}$ , and at higher temperatures the o-wave is now the idler and e-wave is the signal.

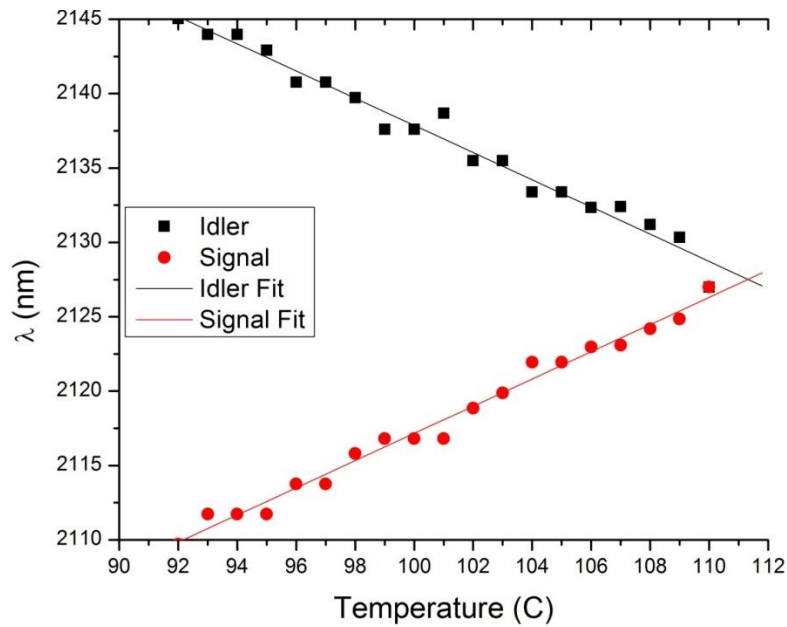


Figure 2. Temperature tuning curve of the OPO. Symbols are data points, solid lines are linear fits.

In addition to monitoring the spectrum, it is beneficial to know the intracavity power. A calibrated InGaAs photodiode was used to monitor the IR power leaking through M4, and the output voltage was proportional to the power circulating in the cavity. The detector was calibrated as follows: One of the high-reflecting cavity mirrors was replaced with a well-calibrated 3% output coupler, and the output power was measured with a power meter. A simultaneous measurement of the voltage on D1 was recorded for a series of signal/idler wavelengths. The intracavity power was determined by using the known transmission curve of the output coupler, giving the detector calibration to within an estimated 10%. Using this calibration, we have estimated greater than 100 W of optical power circulating in the OPO for an empty cavity (no GaAs present), and over 80 W with a GaAs sample. This slight reduction in power is assigned to the additional loss from the sample, which is calculated to be approximately 1.5%.

For maximum THz production, it is important to have signal and idler pulses temporally overlapped at the GaAs. A cross-correlation measurement was taken to determine the signal and idler pulse widths, as well as the relative timing between signal and idler pulses. A small portion of the pump beam was picked off before the OPO and passed through a movable delay line, after which it was combined with signal and idler pulses leaking through M6 on a dichroic mirror. The pulses were then focused into a PPLN crystal, with poling period matched to give efficient sum frequency generation between pump and signal/idler pulses. A half-waveplate inserted before the DCM allowed for the selection of signal or idler for the cross-correlation. After the crystal, a bandpass filter was used to isolate the SFG signal, which was detected with a silicon detector. Results of the measurement are shown in figure 3. Nearly exact overlap is achieved as the GaAs. After deconvolution with the pump width (6 ps), the signal and idler pulses were measured to be ~6.5 ps in duration.

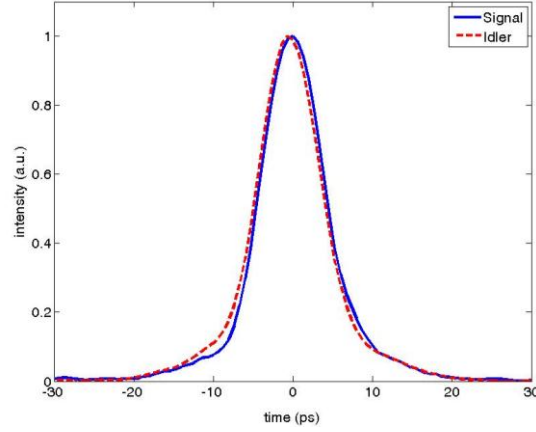


Figure 2. OPO setup. M1 and M2 curved mirrors R = 200 mm. M4 and M5 curved mirrors R = 500 mm. CB = birefringence compensation block. W = wedges. DCM = dichroic mirror. L1, L2, lenses. OAP = off-axis parabolic mirror. BPF = bandpass filter. D1 = InGaAs photodiode. D2 = Si photodiode. FCS = fiber coupled spectrometer.

### 3. GALIUM ARSENIDE SAMPLES

The inherently low efficiency of THz generation by down conversion make the choice of nonlinear crystal important for high power sources. GaAs is an attractive material, as it has many advantageous properties. For DFG with focused picosecond pulses, the conversion efficiency (defined as the ration of THz power to the power in one of the optical pump beams) is proportional to [5]

$$\eta \propto \frac{\omega_{THz}^3 d_{eff}^2}{\Delta n} U_{pump} \quad (1)$$

Here  $\omega_{THz}$  is the THz frequency,  $d_{eff}$  is the effective nonlinear coefficient,  $\Delta n$  is the mismatch between the optical group index and THz phase index, and  $U_{pump}$  is the energy in one of the pump beams. As explained above, high pump energies are achieved by resonant enhancement inside of an optical cavity. GaAs has a low index mismatch ( $\sim 0.18$  at  $2.1 \mu\text{m}$  pump wavelength), and a relatively high nonlinear coefficient ( $d_{14} = 46.1 \text{ pm/V}$ ), which contributes to high efficiency. Additionally, it has a low THz absorption coefficient ( $1 \text{ cm}^{-1}$  in the 1-2 THz range), so that most of the radiation will make it out of the crystal unattenuated. The choice of  $2.1 \mu\text{m}$  for the pump beam is below the energy for 2-photon absorption in GaAs, minimizing loss from nonlinear effects [6].

In order to increase the interaction length, quasi-phasematched structures must be used. At Microtech Instruments we have a semi-automated method to create optically contacted samples by taking individual GaAs wafers and aligning them such that the orientation of the crystal axis alternates with each wafer. This has the effect of changing the phase of the nonlinear polarization, which allows the THz field to increase with increasing sample length. The peak frequency for the efficient generation of THz is given by

$$\omega_0 = \frac{2\pi c}{\Lambda \Delta n} \quad (2)$$

and phase matching acceptance bandwidth is given by

$$\Delta\omega = \frac{2\pi c}{L\Delta n} \quad (3)$$

where  $\Lambda$  is the period of the QPM structure (twice the thickness of an individual wafer) and  $L$  is the length of the sample. Two different samples were used for THz production. The first sample was a single wafer, 0.5 mm thick. The second was a stack of 4x1.0mm wafers. The corresponding peak THz frequencies were 1.5 THz and 0.8 THz, with respective acceptance bandwidths were 3.1 THz and 390 GHz.

## 4. RESULTS

### 4.1 Power Measurements

Samples were inserted at the second focus in the cavity, and the THz power coupled out of the cavity was measured with a calibrated Golay cell (Microtech Instruments). A low pass filter was used to remove any IR and visible radiation, and the beam was chopped at 10 Hz before being focused onto the Golay cell with a 50 mm Tsurupica lens. Additionally an attenuator that blocked 90% of the THz radiation was used to avoid saturation of the Golay cell.

The single wafer sample was used for test purposes, as the broad acceptance bandwidth produces THz for nearly all frequencies reachable by the OPO. When signal and idler pulses were tuned to give a difference of 1.5 THz, this sample produced a maximum of 15  $\mu$ W of THz power with 90 W of power in the cavity. For the 4 layer sample, the maximum THz power was reached with signal and idler tuned to a difference frequency of 0.86THz. The maximum average power of 140  $\mu$ W was measured with 80 W circulating in the cavity. This was within a factor of 2 of the power calculated using the theory of Vodpyanov [4]. When compared with the empty cavity, insertion of the GaAs produced slightly less circulating optical power due to an increase in loss. From a measurement of pump depletion and intracavity power, this gave an increase in loss of 0.5% and 1.2% respectively.

### 4.2 Spectral Measurements

Spectral measurements of the generated THz were done using a Michelson interferometer. The collimated THz beam was incident on a 25  $\mu$ m thick mylar sheet, which served as a beam splitter. Half of the beam was reflected off of a fixed metal mirror, while the other was incident on a mirror mounted on a delay stage. After recombination on the beam-splitter, the beams were focused onto a Golay cell. The THz intensity was recorded step-wise as the delay stage was scanned, and the resulting interferogram was Fourier transformed to give the power spectrum. In figure 4 we show results of the spectral measurements, as well as showing the simultaneous spectrum of the signal and idler from the OPO.

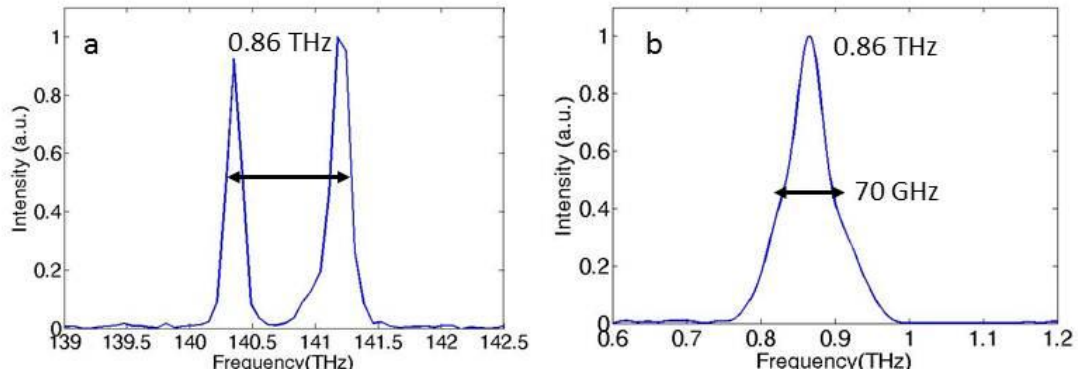


Figure 4. Spectral Measurements, a) OPO spectrum corresponding to b) THz spectrum with sample B. c) OPO spectrum corresponding to c) THz spectrum with sample C.

In fig 4a, we see the signal and idler have a difference of 0.86 THz. The corresponding THz spectrum taken with sample B is shown in fig. 4b, which shows a peak at 0.86 THz. We note that the THz spectrum is centered at the expected frequency determined by the optical spectra. The spectrum is centered near the center frequency determined by the QPM period of the sample (0.79 THz), with the slight differences well within the acceptance bandwidth (390 GHz). The linewidth of the THz pulses is 70 GHz, which corresponds to a temporal width of  $\sim 6$ ps. This short pulse means that as well as high average power, high peak power is also generated ( $>150$  mW peak power for 100  $\mu$ W average power). Furthermore we see that the 70 GHz bandwidth is much narrower than the acceptance bandwidth, but is the same as the  $\sim 70$ GHz bandwidth of the pump pulses. This shows that the pump bandwidth is the limiting factor for THz bandwidth, and longer samples can be used to give more power without loss of bandwidth. We also note that the particular combination of center frequency and linewidth fit well within the atmospheric transmission window at 0.85 THz.

### 4.3 Power Scaling

As higher power pump sources become more readily available, how the scaling of the system scales with pump power is of interest. The scaling of OPO cavity power, and generated THz power with cavity power was therefore investigated. The results of this are shown below, with sample B used in the cavity. Figure 5a shows the scaling of the intracavity power with the pump power, which shows the expected linear scaling and a maximum of 80 W with 5 W pump. Figure 5b shows a log-log plot of the THz power vs. the cavity power, with a maximum of 140  $\mu$ W with 80 W intracavity power. A linear fit gives a slope of 1.8 which is close to the expected quadratic scaling. This scaling, along with the fact that there is no point of THz power saturation, means that a great increase in THz power can be achieved with a modest increase in pump power.

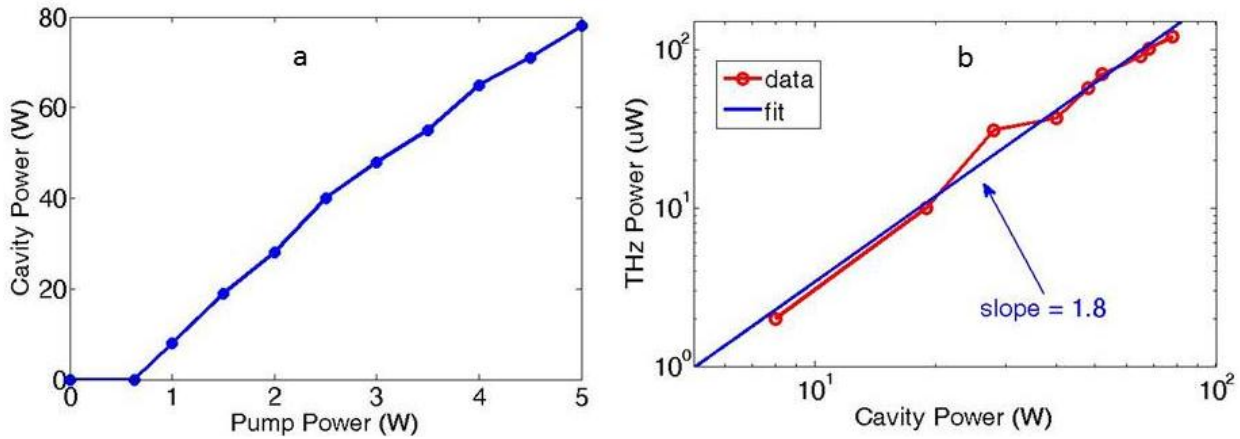


Figure 5. a) Scaling of cavity power with pump power. b) scaling of THz power with cavity power.

## 5. OUTLOOK

### 5.1 Application – Nonlinear imaging

The spectral properties and high average power make this a good source for imaging through the direct detection of the THz signal intensity. In figure 6a we show a schematic for direct imaging of an object by detecting the THz signal. A narrowband THz beam is propagated a distance through the air, reflected off of an object, and then imaged onto a microbolometer array. The high peak power also makes it an attractive option for use in an imaging system employing non-linear detection. In figure 6b we illustrate the proposed method for nonlinear imaging. As in the direct imaging case, a THz beam is propagated through air and reflected from an object. However, instead of directly detecting the THz beam, it is first mixed with an optical beam in a nonlinear crystal, where it is upconverted to an optical signal. This beam is then be imaged with a relatively inexpensive silicon array detector. The isolation of the small upconverted signal from the large optical background is possible due to the narrow spectrum of the THz pulse. Unlike broad bandwidth THz sources [7], the upconverted signal will have no spectral overlap with the optical background, allowing filters to remove the background without attenuating the signal. For example, using a 1.5 THz source for imaging and upconverting with a 1064 nm pulse produces a signal at 1058 nm. This is easily separated from the 1064 nm background with an appropriate low pass filter. Additional isolation can be provided with polarizers, as the upconverted signal is orthogonally polarized with respect to the pump beam.

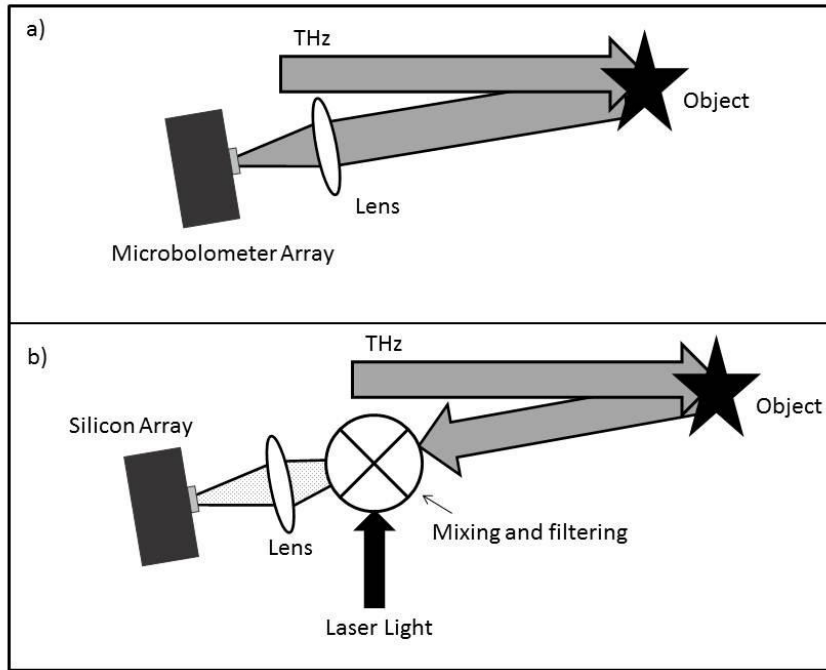


Figure 6: a) direct imaging with microbolometer array b) nonlinear imaging by upconversion of THz pulse with optical pulse and detecting with a silicon array.

## 5.2 Summary

We have demonstrated a narrow linewidth (70 GHz), high average power ( $>100 \mu\text{W}$ ), high peak power ( $>150 \text{ mW}$ ) THz source based on intracavity DFG in QPM GaAs. The type-II ring cavity design allows us to avoid some of the previous complications of the type-II linear cavity and the type-0 ring cavity. The narrow linewidth makes it possible to tune to an atmospheric transmission window where propagation over long distances is possible with minimal attenuation. Sufficient average power is generated to make direct THz imaging possible, while the high peak power due to short pulses makes nonlinear imaging an attractive possibility. We have seen no evidence of saturation of the THz with pump power, showing a clear path to a mW level source higher power pump sources. As the bandwidth appears to depend only on the pump pulse bandwidth, longer samples can be created before the acceptance bandwidth is on the order of the pump bandwidth, allowing for higher power THz generation. With further development higher powers are possible, the current power levels are sufficient for the commercialization of this design, which is now available as a product from Microtech Instruments.

## REFERENCES

- [1] Lee, Y.-S., Hurlbut, W. C., Vodopyanov, K. L., Fejer, M. M., Kozlov, V. G., "Generation of multicycle terahertz pulses via optical rectification in periodically inverted GaAs structures", *Appl. Phys. Lett.* 89, 181104 (2006)
- [2] Schaar, J. E., Vodopyanov, K. L., Fejer, M. M., "Intracavity terahertz-wave generation in a synchronously pumped optical parametric oscillator using quasi-phase-matched GaAs", *Opt. Lett.* 32, 1284 (2007)
- [3] Vodopyanov, K. L., Hurlbut, W. C., Kozlov, V. G., "Photonic THz generation in GaAs via resonantly enhanced intracavity multispectral mixing", *Appl. Phys. Lett.* 99, 041104 (2011)
- [4] Hansen, P. L., Buchhave, P., "Thermal self-frequency locking of a doubly resonant optical parametric oscillator", *Opt. Lett.* 22, 1074-1076 (1997).
- [5] Vodopyanov, K. L., "Optical generation of narrow-band terahertz packets in periodically-inverted electro-optic crystals: conversion efficiency and optimal laser pulse format", *Opt. Lett.* 14, 2263-2276 (2006)



- [6] Hurlbut, W. C., Lee, Y.-S., Vodopyanov, K. L., Kuo, P. S., Fejer, M. M., "Multiphoton absorption and nonlinear refraction of GaAs in the mid-infrared", *Opt. Lett.*, 32, 668 (2007)
- [7] Wu, Q., Hewitt, T. D., Zhang, X.-C., "Two-dimensional electro-optic imaging of THz beams", *Appl. Phys. Lett.* 69, 1026 (1996)